Sequential Phase Linking : Progressive Integration of SAR Images for Operational Phase Estimation

Dana El Hajjar, Yajing Yan, Guillaume Ginolhac, Mohammed Nabil El Korso

SEQUENTIAL PHASE LINKING : PROGRESSIVE INTEGRATION OF SAR IMAGES FOR OPERATIONAL PHASE ESTIMATION

Dana EL HAJJAR[1,2], *Yajing YAN*[1], *Guillaume GINOLHAC*[1], and *Mohammed Nabil EL KORSO*[2]

[1]Université Savoie Mont Blanc, LISTIC, F-74000 Annecy, France
[2]Université Paris-Saclay, CentraleSupélec, L2S, Gif-sur-Yvette, France

ABSTRACT

This paper introduces a novel approach for sequential estimation of the interferometric phase in the context of long Synthetic Aperture Radar (SAR) image time series. When newly acquired data arrive, the data set expands and can be partitioned into two distinct blocks. One represents the previous SAR images and the other represents the newly acquired data. The proposed approach (S-MLE-PL) exploits sequential maximum likelihood estimation of the covariance matrix of the whole data set, taking the existing data set as prior information. This approach facilitates the continuous interferometric phase estimation by incorporating the new data into the previous context. In addition, it presents the advantage of reduced computation time compared to the traditional approaches, making it a more efficient solution for operational displacement estimation.

Index Terms— Multi-temporal InSAR, sequential estimation, covariance matrix, phase linking

1. INTRODUCTION

In recent decades, remote sensing community has witnessed remarkable revolutions in terms of monitoring ground surface deformations over time thanks to the increasing number of Multi-Temporal Interferometric Synthetic Aperture Radar (MT-InSAR) analysis [1]. This advancement results from the evolution of the large amount of available SAR images due to the growing number of launched SAR satellites. One crucial family of approach in MT-InSAR analysis is Distributed Scatterer Interferometry (DSI) which exploits groups of homogeneous scatterers called Distributed Scatterer (DS). Among the multiple DSI approaches, Phase Linking (PL) exploits all possible combinations of SAR images. A set of PL algorithms have been developped among which we can mention: SqueeSAR [2], Eigendecomposition based Maximum likelihood estimator of Interferometric phase (EMI) [3], Phase Linking based on Maximum Likelihood Estimation (MLE-PL) [4, 5]. The main advantage of these approaches is that they consider target statistics through the coherence of interferograms in a rigorous mathematical framework and they allow avoiding phase bias induced by short-lived fading signals present in short temporal baseline interferograms [6].

Thanks to the ongoing and upcoming SAR missions coupled with small revisit cycles (e.g., Sentinel-1 mission $6-12$ days), it becomes possible to acquire unprecedented volumes of SAR data. Moreover, achieving Near Real Time (NRT) monitoring has become a promising goal of InSAR applications, especially for its use in early warnings systems. Traditional MT-InSAR would be unable to incorporate efficiently the newly acquired data and may require replaying the algorithm on the whole dataset. The literature has, to the best of our knowledge, not extensively explored sequential processing of SAR data, as indicated by the limited number of studies addressing this specific topic exploiting PL approaches. The most known sequential approach was developed in [7] where the main idea is to partition the entire stack of SAR images into m mini-stacks. The algorithm starts by treating the first mini-stack and then compressing it into a single virtual image through principal component analysis (PCA). The virtual image obtained is then connected to the next mini-stack, and so on. This approach requires an extended period to form the adequate mini-stack and is based on the standard PL.

In this work, we are interested in developing a sequential approach based on the joint MLE proposed in [4] which presents better performance and has the ability to deal with non-Gaussian data distribution. The previous image stack is taken as prior information, and our approach retrieve the distribution of the new image conditionally to this previous stack. The coherence and the phase difference of the new image with respect to the reference are retrieved using a Block Coordinate Descent (BCD) algorithm. The relevance of the proposed approach is first assessed on synthetic simulations,

The source code is available on GitHub at the following address: https://github.com/DanaElhajjar/S-G-MLE-PL

then on 20 Sentinel-1 SAR images acquired between 14 August 2019 and 10 April 2020 over Mexico city.

2. SEQUENTIAL PHASE LINKING

We consider a stack of $l = p + 1$ SAR images, for a given pixel, we denote $\{\tilde{\mathbf{x}}^i\}_{i=1}^n$ the local homogeneous spatial neighborhood of size n, where $\tilde{\mathbf{x}}^i \in \mathbb{C}^l$, for all $i \in [\![1, n]\!]$, i.e.,

$$\tilde{\mathbf{x}}^i = [\underbrace{x_1^i, \ldots, x_p^i}_{\mathbf{x}^i}, x_l^i]^T \in \mathbb{C}^l \tag{1}$$

where $\mathbf{x}^i \in \mathbb{C}^p$ denotes the multivariate pixel of the previous data (Fig. 1). Each pixel of the local patch is assumed to be distributed as a zero mean Complex Circular Gaussian (CCG) [8], i.e., $\tilde{\mathbf{x}} \sim \mathcal{CN}(0, \tilde{\mathbf{\Sigma}})$.

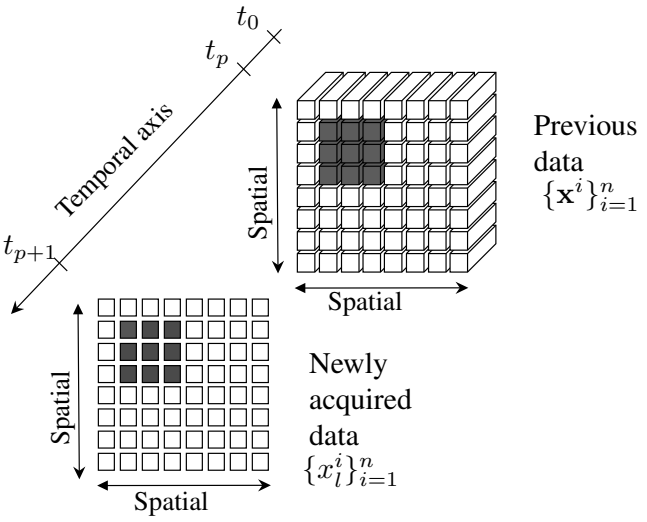

Fig. 1: SAR data representation including both previous and recently obtained images. The local neighborhood of size n is denoted by gray pixels (sliding window).

2.1. Background

Taking into account the phase closure property of the InSAR stack, the covariance matrix of SAR images adheres to the following structure:

$$\tilde{\mathbf{\Sigma}} = \tilde{\mathbf{\Psi}} \odot \tilde{\mathbf{w}}_\theta \tilde{\mathbf{w}}_\theta^H \tag{2}$$

where the symbol $\odot$ represents the element-wise (Hadamard) multiplication, the exponent ^{H} is the transposed and complex conjugated operator (Hermitian), $\tilde{\mathbf{\Psi}}$ is the real core of the covariance matrix and $\tilde{\mathbf{w}}_\theta$ denotes the vector of the exponential of the complex phases ($\tilde{\mathbf{w}}_\theta = [e^{j\theta_0}, \ldots, e^{j\theta_l}]$). The main idea of PL is to estimate $\tilde{\mathbf{\Sigma}}$ which amounts to estimate $\tilde{\mathbf{\Psi}}$ and $\tilde{\mathbf{w}}_\theta$ since the covariance matrix is connected to the unknown coherence matrix and phases, according to (2). PL algorithms are summarized in [9] and compared mathematically in [10]. The standard PL consists of 2 steps : *i*) computing the Sample Covariance Matrix (SCM) over a local patch of the image and then *ii*) considering the plug-in estimate of the coherence matrix $\tilde{\mathbf{\Psi}} = |\text{SCM}|$ and solving the following optimization problem

$$\underset{\tilde{\mathbf{w}}_\theta}{\text{minimize}} \quad \mathcal{L}(|\text{SCM}| \odot \tilde{\mathbf{w}}_\theta \tilde{\mathbf{w}}_\theta^H) \tag{3}$$

where $\mathcal{L}$ corresponds to the negative log-likelihood function of the data following the zero mean CCG distribution. This 2-step approach relies on the plug-in estimate of the coherence matrix which renders it non optimal due to the bias associated with this plug-in. That is why [4, 11] proposed to estimate jointly $\tilde{\mathbf{\Psi}}$ and $\tilde{\mathbf{w}}_\theta$. Therefore, the optimization problem transforms into

$$\begin{aligned} \underset{\tilde{\mathbf{w}}_\theta}{\text{minimize}} \quad & \mathcal{L}(\tilde{\mathbf{\Psi}} \odot \tilde{\mathbf{w}}_\theta \tilde{\mathbf{w}}_\theta^H) \\ \text{subject to} \quad & \tilde{\mathbf{\Psi}} \text{ real}, \ \tilde{\mathbf{w}}_\theta \in \mathbb{T}_l, \ , \ \theta_1 = 0 \end{aligned} \tag{4}$$

where $\mathbb{T}_l = \left\{\tilde{\mathbf{w}} \in \mathbb{C}^l \,|\, |[\tilde{w}]_i| = 1, \forall i \in [1, l]\right\}$ is the l-torus of phase only complex vectors.

2.2. Covariance matrix structure with new data

The hermitian structured covariance matrix, given in (2), can be rewritten as

$$\tilde{\mathbf{\Sigma}} = \begin{pmatrix} \mathbf{\Sigma} & w_{\theta_l}^* diag(\mathbf{w}_\theta) \boldsymbol{\gamma}^T \\ \boldsymbol{\gamma} diag(\mathbf{w}_\theta)^H w_{\theta_l} & \gamma_l \end{pmatrix} \tag{5}$$

where the exponent * is the conjugated operator, $\mathbf{\Sigma}$ denotes the previously estimated covariance matrix between the previous SAR images, $\boldsymbol{\gamma}$ corresponds to the coherence vector between the newly acquired data and the previous ones, γ_l represents the variance of the newly acquired data, and w_{θ_l} is the exponential of the phase of the latest data. We note that 3 parameters associated with the new image are unknown and the remaining are estimated based on the methodology presented in [4]. These parameters will be represented by hats to indicate that they have already been estimated.

2.3. MLE problem

Considering the covariance matrix structure in (5) and assuming that $\{\tilde{\mathbf{x}}^i\}_{i=1}^n$ follows a CCG distribution, the associated negative log-likelihood for the entire data set, can be expressed as:

$$\mathcal{L}_G(\boldsymbol{\gamma}, \gamma_l, w_{\theta_l}) = -\sum_{i=1}^n \mathcal{L}_G^i(x_{p+1}^i | \mathbf{x}^i; \boldsymbol{\gamma}, \gamma_l, w_{\theta_l}) + \mathcal{L}_G^i(\mathbf{x}^i) \tag{6}$$

According to [12], $x_{p+1}^i | \mathbf{x}^i \sim \mathcal{CN}(\mu_x^i, \sigma_x^2)$ where
$\mu_x^i = w_{\theta_l} \boldsymbol{\gamma} \text{diag}(\hat{\mathbf{w}}_\theta)^H \hat{\mathbf{\Sigma}}^{-1} \mathbf{x}^i$
and $\sigma_x^2 = \gamma_l - \boldsymbol{\gamma} \text{diag}(\hat{\mathbf{w}}_\theta)^H \hat{\mathbf{\Sigma}}^{-1} \text{diag}(\hat{\mathbf{w}}_\theta^H) \boldsymbol{\gamma}^T$, and the negative log-likelihood in (6), can be formulated as

$$\mathcal{L}_G(\boldsymbol{\gamma}, \gamma_l, w_{\theta_l}) \propto n \log(v) + \sum_{i=1}^n \frac{y^{i*} y^i}{v}. \tag{7}$$

where $y^i = x_l^i - w_{\theta_l}\,\boldsymbol{\gamma}\,\mathrm{diag}(\hat{\mathbf{w}}_\theta)^H\hat{\boldsymbol{\Sigma}}^{-1}\mathbf{x}^i$
and $v = \gamma_l - \boldsymbol{\gamma}\,\mathrm{diag}(\hat{\mathbf{w}}_\theta)^H\hat{\boldsymbol{\Sigma}}^{-1}\mathrm{diag}(\hat{\mathbf{w}}_\theta)\boldsymbol{\gamma}^T$

In this work, we propose to estimate simultaneously the coherence and the new phase difference using the covariance matrix structure (5),

$$\begin{aligned} \min_{\boldsymbol{\gamma},\gamma_l,\theta_l} \quad & \mathcal{L}_G(\boldsymbol{\gamma},\gamma_l,w_{\theta_l}) \\ \text{subject to} \quad & \boldsymbol{\gamma},\gamma_l \text{ real},\ |w_{\theta_l}| = 1,\ \theta_1 = 0 \end{aligned} \tag{8}$$

The optimization of $\mathcal{L}_G$, defined in (6), will be addressed in a unified manner using a BCD algorithm. The main idea of this algorithm involves estimating each parameter iteratively while fixing the others. Thus, each update corresponds to an optimization sub-problem (cf. Algorithm 1).

Update $\boldsymbol{\gamma}$

Let us start by updating $\boldsymbol{\gamma}$ by solving the following sub-problem

$$\min_{\boldsymbol{\gamma}} \quad \mathcal{L}_G(\boldsymbol{\gamma}) \quad \text{s.t.} \quad \boldsymbol{\gamma} \text{ real} \tag{9}$$

This optimization can be analytically solved as

$$\boldsymbol{\gamma} = \left(\sum_{i=1}^n w_{\theta_l}^* x_l^i \mathbf{L}^i - w_{\theta_l} x_l^{i*}\mathbf{L}^{i*}\right).\left(\sum_{i=1}^n \mathbf{M}^i + \mathbf{M}^{i*}\right)^{-1} \tag{10}$$

where $\mathbf{L}^i = \mathbf{x}^{iH}\hat{\boldsymbol{\Sigma}}^{-1}\mathrm{diag}(\hat{\mathbf{w}}_\theta)$ and $\mathbf{M}^i = \mathbf{L}^{iH}\mathbf{L}^i$

Update γ_l

γ_l is updated by minimizing $\mathcal{L}_G$ while fixing $\boldsymbol{\gamma}$ and w_{θ_l}

$$\min_{\gamma_l} \quad \mathcal{L}_G(\gamma_l) \quad \text{s.t.} \quad \gamma_l \text{ real} \tag{11}$$

The variance of the newly acquired data is calculated as

$$\gamma_l = \frac{1}{n}\sum_{i=1}^n (x_l^i - w_{\theta_l}\boldsymbol{\gamma}\mathbf{L}^{iH})^*(x_l^i - w_{\theta_l}\boldsymbol{\gamma}\mathbf{L}^{iH}) + \boldsymbol{\gamma}\mathbf{N}\boldsymbol{\gamma}^T \tag{12}$$

where $\mathbf{N} = \mathrm{diag}(\hat{\mathbf{w}}_\theta)^H\hat{\boldsymbol{\Sigma}}^{-1}\mathrm{diag}(\hat{\mathbf{w}}_\theta)$

Update w_{θ_l}

The phase difference of the newly acquired SAR image is obtained by solving the following sub-problem

$$\min_{w_{\theta_l}} \quad \mathcal{L}_G(w_{\theta_l}) \quad \text{s.t.} \quad |w_{\theta_l}| = 1,\ \theta_1 = 0 \tag{13}$$

As a result, the phase difference of the newly acquired images takes the following form

$$w_{\theta_l} = \frac{\left(\left(\sum_{i=1}^n x_l^i\mathbf{L}^i\boldsymbol{\gamma}^T\right).\left(\sum_{i=1}^n \boldsymbol{\gamma}\mathbf{M}^i\boldsymbol{\gamma}^T\right)^{-1}\right)}{\left|\left|\left(\left(\sum_{i=1}^n x_l^i\mathbf{L}^i\boldsymbol{\gamma}^T\right).\left(\sum_{i=1}^n \boldsymbol{\gamma}\mathbf{M}^i\boldsymbol{\gamma}^T\right)^{-1}\right)\right|\right|} \tag{14}$$

3. SIMULATIONS

3.1. Simulation parameters

We simulate a time series of size $l = p+1 = 20$ images. The real core of the covariance matrix $\tilde{\boldsymbol{\Psi}}$ is simulated as a Toeplitz matrix i.e., $[\tilde{\boldsymbol{\Psi}}]_{ij} = \rho^{|i-j|}$ with a coefficient correlation $\rho = 0.7$. $\boldsymbol{\gamma}$ corresponds to the last raw of this matrix and

Algorithm 1 BCD algorithm

1: **Input**: Samples $\{\tilde{\mathbf{x}}^i\}_{i=1}^n$, $\hat{\boldsymbol{\Sigma}}$, $\mathrm{diag}(\hat{\mathbf{w}}_\theta)$
2: **repeat**
3: Update of $\boldsymbol{\gamma}$ with (10)
4: Update of γ_l with (12)
5: Update of w_{θ_l} with (14)
6: **until** convergence
7: **Output**: $\boldsymbol{\gamma}$, γ_l and w_{θ_l}

γ_l the scalar at (l,l) position. Phases differences vary linearly between 0 and 2 rad, i.e., $\Delta_{i,i-1} = \theta_i - \theta_{i-1} = 2/l$ rad. The covariance matrix is then obtained according to (2) with which we simulate n independent and identically distributed (i.i.d) samples according to the CCG, $\tilde{\mathbf{x}}^i \sim \mathcal{N}(0, \tilde{\boldsymbol{\Sigma}})$. We compare the results of our approach with those obtained from other state-of-the-art approaches: 2-pass InSAR designated hereinafter by 2p-InSAR, which is equivalent to an interferogram between 2 images, standard PL [10] and MLE-PL [11]. Mean Squared Error (MSE) are computed using 1000 Monte Carlo trials.

3.2. Simulation results

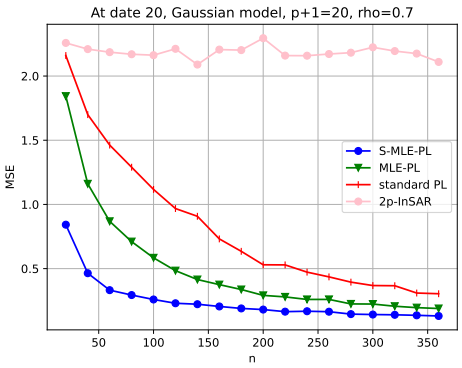

Fig. 2: MSE on w_{θ_l} with increasing n, $l = 20$, $\rho = 0.7$ using 1000 Monte Carlo trials.

Fig. 2 represents the MSE of the phase difference estimate for the latest SAR image when the size of the patch n increases. As expected, the MSE decreases as the number of samples increases.

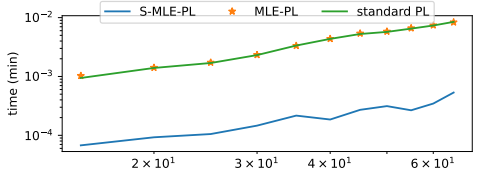

Fig. 3: Comparison of computation time among standard PL, MLE-PL and Sequential Phase Linking based on Maximum Likelihood Estimation (S-MLE-PL).

It is worth noting that the sequential estimation of w_{θ_l} provides better results than other considered approaches. At the core of the sequential approach lies the prior estimation of the past using [11]. Consequently, predicting future outcomes is expected to yield superior results. Fig. 3 presents the computation cost when the length of the time series increases. The primary factor for the heavy computation time of the PL approach is the number of involved images. As the number of images increases, the computational cost also rises due to the processing of the coherence matrix whose size corresponds to the number of involved images. Classic approaches deal with matrices of size (l, l) while our approach treats 2 scalars and a vector of size p. The complexity of the offline algorithm is primarily dominated by matrix inversion and Singular Value Decomposition (SVD), which are performed multiple times (n_{iter} the number of iterations), with a cost of $O(n_{\text{iter}}\, p^3)$. In contrast, the sequential approach requires only one matrix inversion, which amounts to $O(p^3)$.

4. REAL DATA

With a population exceeding 20 million, Mexico city stands as one of the most dynamic cities in the world, coupled with the rapid urbanization which led to a huge demand for water. The primary source of Mexico City's water supply is aquifers, and heavy water pumping is the main factor causing subsidence and deformation over the city [13]. We use a stack of 20 SAR images over the Mexico City acquired every 12 days, from 14 August 2019 to 10 April 2020, corresponding to 8 months to assess the performance of the proposed S-MLE-PL approach. The interferograms estimated by both

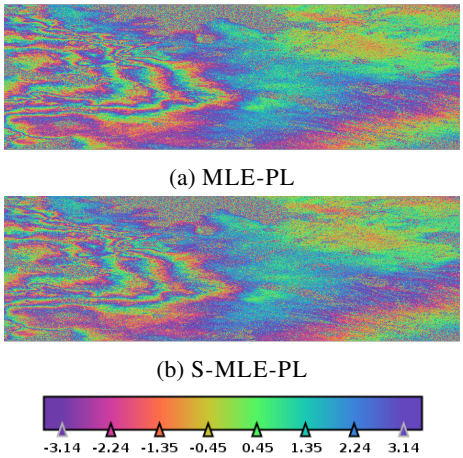

(a) MLE-PL

(b) S-MLE-PL

Fig. 4: Close-up view of interferograms (14 August 2019 - 10 April 2020) estimated by (a) MLE-PL, and (b) S-MLE-PL in case $l = 20$ and $n = 64$

the MLE-PL and the proposed S-MLE-PL approach, are illustrated in Fig 4. In both cases, the multi-looking window, denoted as $n = 8 \times 8$, remains the same. The MLE-PL and S-MLE-PL methods yield the same results, however the sequential approach demonstrates significantly faster execution time than the MLE-PL when applied to real data.

5. CONCLUSION

This paper presents a novel sequential PL approach that allows incorporating efficiently new SAR images in interferometric phase estimation in a PL framework. According to synthetic simulations and real data applications, the proposed S-MLE-PL approach presents the same performance and lower computational cost compared to MLE-PL.

6. ACKNOWLEDGEMENT

This work is funded by the ANR REPED-SARIX project (ANR-21-CE23-0012-01) of the French national Agency of research.

References

[1] B. Osmanoğlu, F. Sunar, S. Wdowinski, and E. Cabral-Cano, "Time series analysis of insar data: Methods and trends," ISPRS Journal of Photogrammetry and Remote Sensing, vol. 115, pp. 90–102, 2016.

[2] A. Ferretti, A. Fumagalli, F. Novali, C. Prati, F. Rocca, and A. Rucci, "A new algorithm for processing interferometric data-stacks: Squeesar," IEEE transactions on geoscience and remote sensing, vol. 49, no. 9, pp. 3460–3470, 2011.

[3] H. Ansari, F. De Zan, and R. Bamler, "Efficient phase estimation for interferogram stacks," IEEE Transactions on Geoscience and Remote Sensing, vol. 56, no. 7, pp. 4109–4125, 2018.

[4] P. Vu, A. Breloy, F. Brigui, Y. Yan, and G. Ginolhac, "Robust phase linking in insar," IEEE Transactions on Geoscience and Remote Sensing, vol. 61, pp. 1–11, 2023.

[5] C. Wang, X. Wang, Y. Xu, Bochen Zhang, M. Jiang, S. Xiong, Q. Zhang, W. Li, and Q. Li, "A new likelihood function for consistent phase series estimation in distributed scatterer interferometry," IEEE Transactions on Geoscience and Remote Sensing, vol. 60, pp. 1–14, 2022.

[6] H. Ansari, F. De Zan, and A. Parizzi, "Study of systematic bias in measuring surface deformation with sar interferometry," IEEE Transactions on Geoscience and Remote Sensing, vol. 59, no. 2, pp. 1285–1301, 2020.

[7] H. Ansari, F. De Zan, and R. Bamler, "Sequential estimator: Toward efficient insar time series analysis," IEEE Transactions on Geoscience and Remote Sensing, vol. 55, no. 10, pp. 5637–5652, 2017.

[8] R. Bamler and P. Hartl, "Synthetic aperture radar interferometry," Inverse problems, vol. 14, no. 4, pp. R1, 1998.

[9] D. Minh and S. Tebaldini, "Interferometric phase linking: Algorithm, application, and perspective," IEEE Geoscience and Remote Sensing Magazine, vol. 11, no. 3, pp. 46–62, 2023.

[10] N. Cao, H. Lee, and H. Jung, "Mathematical framework for phase-triangulation algorithms in distributed-scatterer interferometry," IEEE Geoscience and Remote Sensing Letters, vol. 12, no. 9, pp. 1838–1842, 2015.

[11] P. Vu, F. Brigui, A. Breloy, Y. Yan, and G. Ginolhac, "A new phase linking algorithm for multi-temporal insar based on the maximum likelihood estimator," in IGARSS 2022-2022 IEEE International Geoscience and Remote Sensing Symposium. IEEE, 2022, pp. 76–79.

[12] T. W. Anderson, An introduction to multivariate statistical analysis, vol. 2, Wiley New York, 1958.

[13] Y. Yan, M. Doin, P. Lopez-Quiroz, F. Tupin, B. Fruneau, V. Pinel, and E. Trouvé, "Mexico city subsidence measured by insar time series: Joint analysis using ps and sbas approaches," IEEE Journal of Selected Topics in Applied Earth Observations and Remote Sensing, vol. 5, no. 4, pp. 1312–1326, 2012.